Journal of Solid State Chemistry **158,** 148–153 (2001)
foi:10.1006/jssc.2001.9085, available online at http://www.idealibrary.com on IDEAL®

Crystal Structure and Magnetic Properties of $Li_2Mn_2(SO_4)_3$

J. Isasi

Departamento de Quimica Inorganica I, Facultad de Ciencias Quimicas, Universidad Complutense, 28040 Madrid, Spain

C. Train

Laboratoire de Chimie Inorganique et Matériaux Moléculaires, Université Pierre et Marie Curie — Paris VI, 4 place Jussieu, 75252 Paris Cedex 05, France

and

S. Jaulmes, A. Elfakir, and M. Quarton[1]

Laboratoire de Cristallochimie du Solide, Université Pierre et Marie Curie — Paris VI, 4 place Jussieu, 75252 Paris Cedex 05, France

Received July 12, 2000; in revised form December 14, 2000; accepted January 19, 2001; published online March 27, 2001

The crystal structure of dilithium dimanganese trisulfate $Li_2Mn_2(SO_4)_3$ has been established by single-crystal X-ray diffraction. This compound crystallizes in the orthorhombic system (space group *Pbca*, $Z = 8$) with cell parameters $a = 8.686(2)$ Å, $b = 8.792(2)$ Å, and $c = 24.146(4)$ Å. The structure was refined to $R = 0.035$ and $Rw = 0.037$ using 2622 independent reflections. Lithium and sulfur atoms are in most regular tetrahedral oxygen coordination, manganese atoms are in slightly distorted octahedral oxygen coordination. Formally, the 3-D framework can be described, starting from the $Li_2Mg_2(SO_4)_3$ structure, by condensation of $Sc_2(WO_4)_3$-type slabs. As a result, half of the LiO_4 and MnO_6 polyhedra share an edge, forming Li_2O_6 and Mn_2O_{10} dimeric entities. Below $T_N = 10$ K, the magnetic susceptibility evolution is characteristic of a long-range antiferromagnetic order. In the high-temperature region, the susceptibility follows a Curie–Weiss law with $C = 8.51$ cm^3 K mol^{-1} and $\theta = -19$ K. In a Mn_2O_{10} bioctahedron the Mn^{2+} cations are indeed antiferromagnetically coupled with an interaction parameter $J = -6.5$ cm^{-1}.

INTRODUCTION

Over the past years, the transition metal oxides with layered or 3-D framework structures have been extensively investigated as cathodes materials for secondary Li-batteries (1). Amid them, the Ni, Co, and Mn compounds were highly studied in consideration of their electrochemical performances (2). Recently, some Li intercalation studies in host compounds containing $(XO_4)^{n-}$ polyanions (X = P, As, S, Mo, W) in place of O^{2-} ions pointed out very interesting results (3–8). The large $(XO_4)^{n-}$ polyanions can generate an open 3-D framework with fast mobility of Li^+ ions and they allow one to adapt the Li intercalation–deintercalation process potential. The potential of a redox couple in a given coordination shell is lower in the oxide form than it would be by substituting the oxygen anion by a more electro-attractive anionic structural unit (9).

In order to identify new host compounds for Li intercalation, we have investigated the synthesis, the crystal structure, and the properties of the mixed sulfate $Li_2Mn_2(SO_4)_3$. The results are presented below.

EXPERIMENTAL

The title compound was prepared by solid-state reaction from $Li_2SO_4 \cdot H_2O$ (Prolabo, RP Normapur) and $MnSO_4 \cdot H_2O$ (Prolabo, RP Normapur). Stoichiometric amounts of starting materials were mixed thoroughly in an agate mortar, placed in a platinum crucible, and submitted to heat treatments in air for several hours to remove water. After series of alternate grinding stages (300 to 450°C) the samples were pressed and kept at 500°C in air for 72 h. The completion of the reaction was checked by weighting of the heated samples and by examination of their X-ray powder diffraction patterns. The X-ray diffractograms were registrated with a Philips PW-1050 goniometer using the Fe$K\alpha$ radiation.

Single crystals were grown from the molten compound by slow cooling (5°C h^{-1}) to room temperature. Samples obtained are light brown and transparent.

Several single crystals were selected to record Weissenberg and precession photographs which showed orthorhombic symmetry with extinctions corresponding to the

[1]To whom correspondence should be addressed. E-mail: mg@ccr.jussieu.fr. Fax: 33-1 44 27 25 48.

0022-4596/01 $35.00

TABLE 1
Crystal Data and Data Collection

Crystallographic data	
Chemical formula	$Li_2Mn_2(SO_4)_3$
Molar mass	412.07
Crystal system/space group	Orthorhombic/*Pbca* (no. 61)
Cell parameters	$a = 8.686(2)$ Å
	$b = 8.792(2)$ Å
	$c = 24.146(4)$ Å
	$V = 1844(1)$ Å^3
$D_{mes}/D_{calc}/Z$	3.00(4)/2.969 g cm^{-3}/$Z = 8$
$F(000)$	1600
Data collection and refinement	
Diffractometer	Enraf–Nonius CAD-4
Temperature	293 K
Radiation/wavelength	Mo$K\alpha$/0.71069 Å
Scan mode	$\omega/2\theta$
Scan angle	$0.8 + 0.345$ tg θ
Shape: parallelepiped	$0.094 \times 0.094 \times 0.054$ mm
Number of independent reflections	4036
Reflections with $I > 3\sigma(I)$	2622
Absorption coefficient	34.83 cm^{-1}
Transmission factor extreme values	0.765–0.848
Number of variables	173
R/R_w/weighting scheme	0.035/0.037/w $= 1/\sigma(F)$
Extinction parameter refined	$g = 0.56(7) \times 10^{-6}$
$(\Delta/\sigma)_{max}$	6×10^{-3}
Extreme residual electronic densities	$-0.66/0.39$ eÅ^{-3}

space group *Pbca* (no. 61). The X-ray diffractogram obtained from ground single crystals was comparable with the one of $Li_2Mg_2(SO_4)_3$ (10), suggesting a structural correlation in spite of different space groups for these two compounds.

The experimental conditions of the diffracted intensities collection are listed in Table 1. Crystal morphology and dimensions have been verified from five ψ-scan measurements, then the data were used for absorption corrections with an analytical method (11). The Mn and S atoms were first located by direct methods with MULTAN 88 (12). Electronic density maps obtained from Fourier series gave approximate coordinates of O and Li atoms. Refinements of atomic coordinates were performed by means of the ORXFLS program (13) using atomic scattering factors (14). Secondary extinction corrections showed an isotropic disorientation of type I (15): mosaic crystal with gaussian distribution (standard deviation $\sigma = 10''$).

Magnetic susceptibility was measured from 4 K up to room temperature, using a Manics DSM8 magnetometer, in the magnetic field range 0–17 kOe. The applied diamagnetic correction was equal to -149×10^{-6} cm^3 mol^{-1}.

STRUCTURE DESCRIPTION

The atomic coordinates and equivalent thermal parameters are reported in Table 2. Table 3 gathers the anisotropic displacement parameters; the main values of interatomic distances and interbond angles are given in Table 4.

TABLE 2
Fractional Atomic Coordinates and Thermal Parameters
$U_{eq} = \sum_i \sum_j U_{ij} a_i^* a_j^* a_i . a_j$

Atoms	x	y	z	U_{eq} (Å^2)
Li(1)	0.9626(7)	0.1231(6)	0.2086(3)	0.020(2)
Li(2)	0.3562(7)	0.4312(7)	0.0095(3)	0.021(2)
Mn(1)	0.49785(6)	0.29478(5)	0.17783(2)	0.0116(2)
Mn(2)	0.00116(5)	0.40261(4)	0.06598(2)	0.0093(1)
S(1)	0.85094(7)	0.75291(7)	0.05174(3)	0.0079(2)
S(2)	0.64445(7)	0.94674(7)	0.20128(3)	0.0080(2)
S(3)	0.19450(7)	0.09305(7)	0.11620(3)	0.0099(2)
O(11)	0.6407(3)	0.2318(3)	0.11112(8)	0.167(9)
O(12)	0.5653(2)	0.3877(2)	0.0346(1)	0.0161(9)
O(13)	0.6900(2)	0.7640(2)	0.03321(9)	0.0138(8)
O(14)	0.5844(2)	0.1133(2)	0.02420(8)	0.0122(8)
O(21)	0.5897(3)	0.9159(3)	0.1458(1)	0.024(1)
O(22)	0.8132(2)	0.9562(3)	0.2024(1)	0.0171(9)
O(23)	0.5946(3)	0.8218(2)	0.23787(9)	0.0178(9)
O(24)	0.5810(2)	0.0913(2)	0.22202(9)	0.0125(8)
O(31)	0.3104(3)	0.1779(3)	0.1453(1)	0.034(1)
O(32)	0.0939(3)	0.1892(3)	0.0833(1)	0.028(1)
O(33)	0.0986(3)	0.0120(3)	0.1565(1)	0.022(1)
O(34)	0.2659(3)	0.9825(3)	0.07775(9)	0.0186(9)

The crystal structure forms a 3-D framework built up from LiO_4 and SO_4 tetrahedra and MnO_6 octahedra. The SO_4 tetrahedra are highly regular in agreement with the strongly covalent character of the S–O bonds. The mean length of Mn–O bonds is 2.17 Å (Table 4), it agrees with the

TABLE 3
Anisotropic Displacement Parameters (Å$^2 \times 10^3$) in $Li_2Mn_2(SO_4)_3$

Atom	U_{11}	U_{22}	U_{33}	U_{12}	U_{13}	U_{23}
Li(1)	18(3)	14(3)	28(3)	− 2(2)	3(2)	− 5(2)
Li(2)	20(3)	16(3)	27(3)	− 3(3)	− 2(3)	− 1(2)
Mn(1)	12.5(2)	9.4(1)	12.9(2)	− 0.4(2)	− 0.2(2)	− 1.1(1)
Mn(2)	8.7(1)	8.9(1)	10.3(1)	0.2(1)	− 0.4(1)	0.9(1)
S(1)	7.3(2)	6.8(2)	9.4(2)	0.9(2)	− 0.2(2)	− 1.1(2)
S(2)	8.9(2)	6.5(2)	8.7(2)	0.6(2)	0.4(2)	− 0.2(2)
S(3)	8.5(2)	6.9(2)	14.3(3)	0.1(2)	0.5(2)	1.0(2)
O(11)	20.5(9)	21(1)	9.0(8)	− 0.6(8)	2.2(7)	− 2.9(7)
O(12)	15.4(9)	8.3(8)	25(1)	2.4(7)	− 1.4(8)	− 0.3(7)
O(13)	7.9(7)	16.7(9)	16.9(8)	2.7(7)	− 2.0(6)	− 2.8(7)
O(14)	16.1(8)	9.1(8)	11.4(8)	− 4.6(7)	− 1.6(6)	− 2.5(6)
O(21)	28(2)	29(2)	14.3(9)	8(1)	− 10.1(8)	− 7.5(9)
O(22)	7.8(7)	15.4(8)	28(2)	− 0.4(6)	1.1(8)	− 6.5(8)
O(23)	26(1)	8.1(7)	20(1)	− 3.0(7)	8.2(8)	2.9(7)
O(24)	17.2(9)	6.7(7)	13.5(8)	3.5(7)	3.4(7)	− 0.4(7)
O(31)	26(2)	29(2)	48(2)	− 14(2)	− 13(2)	− 9(2)
O(32)	35(2)	15(1)	34(2)	14(1)	− 11(2)	1.6(9)
O(33)	30(2)	14.5(9)	22(1)	− 7.7(9)	13.6(9)	− 0.9(8)
O(34)	16.1(9)	21(1)	18.9(9)	8.4(8)	4.5(8)	− 3.1(8)

TABLE 4
Interatomic Distances (Å) and Angles (°) for Each Anionic Polyhedra in $Li_2Mn_2(SO_4)_3$

	$S(1)O_4$ tetrahedron – $\langle S(1)–O\rangle = 1.468$ Å					$S(2)O_4$ tetrahedron – $\langle S(2)–O\rangle = 1.466$ Å			
S(1)	O(11)	O(12)	O(13)	O(14)	S(2)	O(21)	O(22)	O(23)	O(24)
O(11)	**1.449(3)**	2.392(4)	2.405(4)	2.394(4)	O(21)	**1.446(3)**	2.400(3)	2.373(4)	2.402(4)
O(12)	111.2(2)	**1.451(3)**	2.388(3)	2.431(3)	O(22)	110.7(2)	**1.471(3)**	2.395(4)	2.388(3)
O(13)	110.9(2)	109.6(2)	**1.470(3)**	2.376(3)	O(23)	108.6(2)	109.0(2)	**1.473(3)**	2.403(3)
O(14)	108.4(2)	110.7(2)	105.9(2)	**1.503(3)**	O(24)	110.7(2)	108.5(2)	109.2(2)	**1.474(3)**

	$S(3)O_4$ tetrahedron – $\langle S(3)–O\rangle = 1.459$ Å			
S(3)	O(31)	O(32)	O(33)	O(34)
O(31)	**1.437(3)**	2.406(4)	2.363(4)	2.400(4)
O(32)	112.8(2)	**1.454(3)**	2.357(4)	2.357(4)
O(33)	109.0(2)	107.7(2)	**1.466(3)**	2.407(4)
O(34)	110.7(2)	106.9(2)	109.7(2)	**1.479(3)**

	$Mn(1)O_6$ octahedron – $\langle Mn(1)–O\rangle = 2.165$ Å					
Mn(1)	O(31)	O(11)	O(33)	O(23)	O(24)	O(22)
O(31)	**2.079(3)**	3.023(6)	3.054(6)	3.200(5)	3.088(5)	4.310(7)
O(11)	92.4(2)	**2.106(3)**	3.404(6)	4.254(6)	2.994(4)	2.985(5)
O(33)	92.5(2)	106.3(1)	**2.148(3)**	3.050(5)	4.315(7)	2.759(4)
O(23)	96.7(2)	161.8(1)	89.0(1)	**2.202(3)**	2.715(4)	3.074(5)
O(24)	92.2(2)	87.9(1)	164.8(1)	76.1(21)	**2.204(3)**	3.371(5)
O(22)	169.2(2)	86.4(1)	77.5(1)	87.4(1)	98.5(1)	**2.248(3)**

	$Mn(2)O_6$ octahedron – $\langle Mn(2)–O\rangle = 2.179$ Å					
Mn(2)	O(32)	O(21)	O(34)	O(13)	O(14)	O(14)
O(32)	**2.085(3)**	2.965(5)	2.855(5)	2.824(5)	4.282(7)	3.124(5)
O(21)	90.7(2)	**2.087(3)**	3.310(5)	3.152(5)	3.411(5)	3.411(5)
O(34)	84.6(2)	102.4(1)	**2.160(3)**	4.292(7)	3.263(5)	2.909(4)
O(13)	82.2(2)	94.4(1)	158.7(1)	**2.207(3)**	3.212(4)	2.961(4)
O(14)	164.7(1)	104.1(1)	95.8(1)	92.7(1)	**2.237(3)**	2.736(4)
O(14)	90.7(1)	176.1(1)	81.4(1)	82.2(1)	74.3(1)	**2.300(3)**

	$Li(1)O_4$ tetrahedron – $\langle Li(1)–O\rangle = 1.970$ Å					$Li(2)O_4$ tetrahedron – $\langle Li(2)–O\rangle = 2.010$ Å			
Li(1)	O(23)	O(22)	O(33)	O(24)	Li(2)	O(12)	O(34)	O(12)	O(13)
O(23)	**1.946(7)**	3.074(5)	3.754(6)	2.715(4)	O(12)	**1.952(8)**	3.171(5)	2.825(4)	3.062(4)
O(22)	122.0(4)	**1.963(7)**	2.759(4)	3.186(5)	O(34)	106.4(4)	**2.009(8)**	3.420(5)	3.509(5)
O(33)	145.5(4)	88.5(3)	**1.984(7)**	3.019(5)	O(12)	90.2(3)	115.5(4)	**2.036(7)**	3.481(4)
O(24)	87.4(3)	107.5(4)	99.0(3)	**1.986(8)**	O(13)	100.2(3)	120.1(4)	117.1(4)	**2.043(7)**

value 2.19 Å equal to the ionic radii sum (16), thus confirming the state of the high-spin manganese(II) cations. The two $Mn(1)O_6$ and $Mn(2)O_6$ octahedra are connected via three bridging SO_4 tetrahedra (Fig. 1), constituting a structural unit $Mn_2S_3O_{18} = M_2X_3O_{18}$, which is well known in the $Sc_2(WO_4)_3$-type compounds (17). In this structural type, the $M_2X_3O_{18}$ "lantern" units are linked together by corner sharing, and interstitial sites are available for A cations, leading to $A_xM_2(XO_4)_3$ compounds such as $Li_2Mg_2(SO_4)_3$ (18).

The crystal structures of $Li_2Mg_2(SO_4)_3$ and $Li_2Mn_2(SO_4)_3$ are compared in Fig. 2. It is clear that the present framework results from the connection of $Sc_2(WO_4)_3$-type slabs by edge-sharing, this involving the doubling of the largest unit-cell parameter. Thus all the $Mn_2S_3O_{18}$ structural units are paired as shown in Fig. 1. The MnO_6 octahedra appear independent for half of them ($Mn(1)O_6$) and involved in bioctahedra for the other half ($Mn(2)O_6$). In correlation, the same repartition is observed for the LiO_4 tetrahedra: all the $Li(1)O_4$ tetrahedra are independent, whereas the $Li(2)O_4$ tetrahedra constitute Li_2O_6 bitetrahedra by edge sharing.

$Li_2Mg_2(SO_4)_3$ presents alternated chains of edge-sharing LiO_4 tetrahedra and MgO_6 octahedra along c (Fig. 2a).

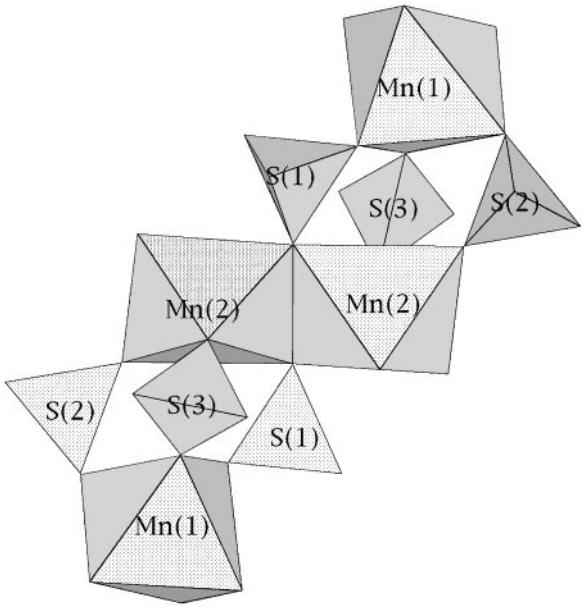

FIG. 1. Two structural units $Mn_2S_3O_{18}$ linked together by edge sharing. Each "lantern" unit is composed of $Mn(1)O_6$ and $Mn(2)O_6$ octahedra bridged by three SO_4 tetrahedra.

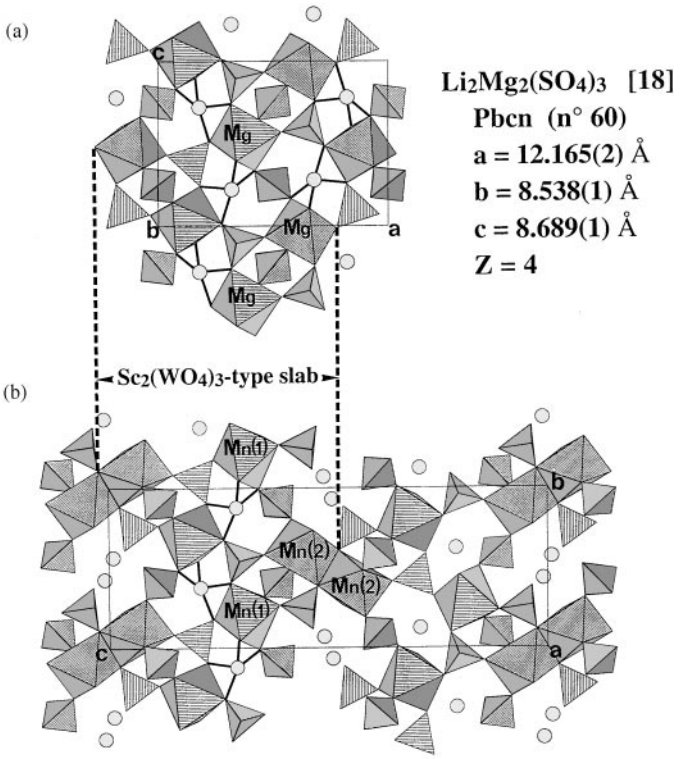

FIG. 2. Cell projections of (a) $Li_2Mg_2(SO_4)_3$ and (b) $Li_2Mn_2(SO_4)_3$ showing the (circles) Li atoms, MgO_6 or MnO_6 octahedra and SO_4 tetrahedra.

$Li_2Mn_2(SO_4)_3$ presents these same independent chains along b for $z \cong \frac{1}{4}$ and $\frac{3}{4}$ (Fig. 3a), but also alternated chains of corner-sharing Li_2O_6 bitetrahedra and Mn_2O_{10} bioctahedra linked together by corner-sharing for $z \cong 0$ and 1/2 (Fig. 3b). These two polyhedra ribbons are interconnected by SO_4 tetrahedra, which then constitutes a 3-D framework.

To our knowledge, the presence of dimeric entities in a $Sc_2(WO_4)_3$-type compound is evidenced for the first time. For each of the Li_2O_6 and Mn_2O_{10} bipolyhedra the common edge constitutes the shortest O–O distance: O(12)–O(12) = 2.825 Å in Li_2O_6 and O(14)–O(14) = 2.736 Å in Mn_2O_{10} (Table 4), which then realizes a screening of Li^+/Li^+ and Mn^{2+}/Mn^{2+} intercationic repulsions. In a Mn_2O_{10} bioctahedron the manganese–manganese distance is 3.617 Å and the two bridging oxygen atoms have longer Mn–O bond lengths than the other oxygen atoms. The Mn–O–Mn angle is 105.8°. Such a geometry with two bridging oxygen atoms allows superexchange magnetic interactions between the $Mn(2)^{2+}$ cations (19, 20).

MAGNETIC PROPERTIES

The experimental $\chi_M^{-1} = f(T)$ variation (Fig. 4) shows the onset of a long-range antiferromagnetic (AF) order at a Néel temperature of 10 K. Above this temperature, the data can be fitted with a Curie–Weiss law, $\chi = C/(T - \theta)$, with a Weiss temperature $\theta = -19$ K and a Curie constant $C = 8.51\ cm^3\ K\ mol^{-1}$. The negative value of θ reveals the existence of AF interactions between the metallic cations. The value of C is slightly lower than the value predicted for two free Mn^{2+} cations per formula unit ($8.75\ cm^3\ K\ mol^{-1}$ assuming $g = 2$).

The $\chi_M T$ versus T curve (Fig. 5) decreases monotonically when the temperature is lowered. This confirms the existence of AF interactions between the metallic ions. The crystallographic results show that only half of the manganese(II) are oxygen-bridged while for the other half, such an efficient exchange pathway does not exist. A $Li_4Mn_4(SO_4)_6$ unit thus includes two magnetically uncoupled $Mn(1)^{2+}$ ions and two interacting $Mn(2)^{2+}$ ions. Using the exchange Hamiltonian $-J\hat{S}_{Mn^{2+}}\hat{S}_{Mn^{2+}}$ for the latter ions, the susceptibility of the system then writes (21)

$$\chi = 2\,\frac{N\beta^2 g^2}{kT} \times \left(\frac{S(S+1)}{3} + \frac{e^x + 5e^{3x} + 14e^{6x} + 30e^{10x} + 55e^{15x}}{1 + 3e^x + 5e^{3x} + 7e^{6x} + 9e^{10x} + 11e^{15x}} \right)$$

with N the Avogadro constant, k the Boltzman constant, β the Bohr magneton, g an average Landé factor, S equals $\frac{5}{2}$, and $x = J/kT$. Least-squares fitting of $\chi_M T$ between 30 and 290 K leads to $J = -6.5\ cm^{-1}$ and $g = 1.96$ with $R = \sum[(\chi^{obs}T - \chi^{calc}T)^2/(\chi^{obs}T)^2] = 0.2\%$.

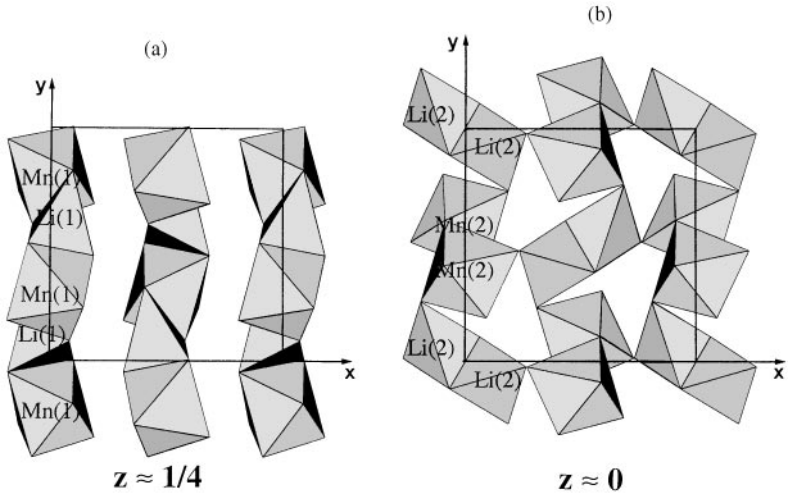

FIG. 3. Alternated chains along [010] made up (a) from $Li(1)O_4$ tetrahedra and $Mn(1)O_6$ octahedra and (b) from $Li(2)_2O_6$ bitetrahedra and $Mn(2)_2O_{10}$ bioctahedra.

In order to discuss the relevance of these values, a comparison has been made between the present Mn_2O_{10} dimer and manganese(II) dimers with oxygen containing bridges which have been structurally and magnetically characterized (22, 23). Owing to the fact that many structural parameters are different from those measured here, the value found for J is in accordance with those previously reported.

CONCLUSION

On the basis of their similar X-ray diffractograms, the $Li_2Mg_2(SO_4)_3$ and $Li_2Mn_2(SO_4)_3$ sulfates appear as isotypic compounds. In fact, their 3-D structural skeletons adopt the $Sc_2(WO_4)_3$-type but in $Li_2Mn_2(SO_4)_3$ the slabs are associated by edge-sharing instead of corner-sharing. This connection mode results in the doubling of the largest unit-cell parameter and a different orthorhombic space group.

The main feature of this crystal structure is the presence of Li_2O_6 bitetrahedra and Mn_2O_{10} bioctahedra. The antiferromagnetic coupling between Mn^{2+} cations in the dimeric Mn_2O_{10} entities leads to a stabilizing energy which can explain the original structure of $Li_2Mn_2(SO_4)_3$.

Tests of lithium electrochemical deintercalation were performed in galvanostatic mode using a MacPile system at a C/50 rate within a 3.0–4.3 V potential window vs Li^+/Li. These tests were unfruitful because the lithium ions were trapped in two different tetrahedral sites and they could not be extracted from $Li_2Mn_2(SO_4)_3$. This result is in agreement with the structural arrangement of the $Sc_2(WO_4)_3$-type compounds which are poor ionic conductors (24).

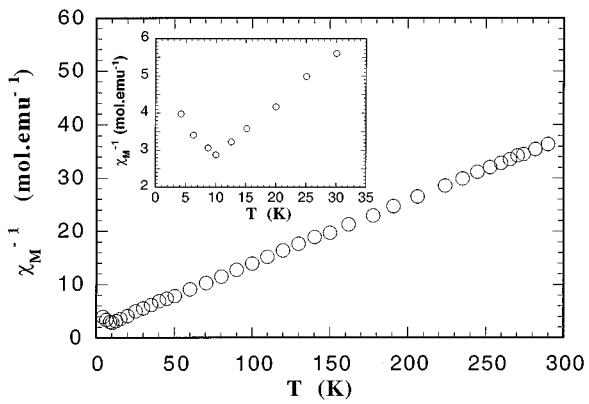

FIG. 4. Thermal variation of the reciprocal molar magnetic susceptibility of $Li_2Mn_2(SO_4)_3$.

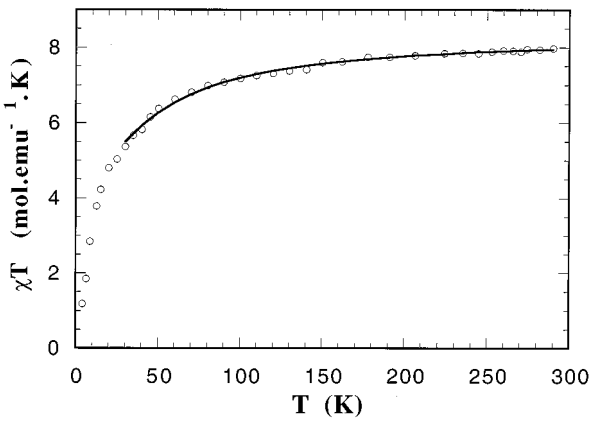

FIG. 5. Thermal variation of the magnetic susceptibility × temperature product in $Li_2Mn_2(SO_4)_3$: (circles) experimental data and (full line) calculated values above 30 K.

ACKNOWLEDGMENT

The authors thank N. Dupont for performing the magnetic susceptibility measurements.

REFERENCES

1. M. Winter, J. O. Besenhard, M. E. Spahr, and P. Novak, *Adv. Mater.* **10,** 725 (1998).
2. C. Delmas, M. Ménétrier, L. Croguennec, S. Levasseur, J. P. Pérès, C. Pouillerie, G. Prado, L. Fournès, and F. Weill, *Int. J. Inorg. Mater.* **1,** 11 (1999).
3. J. Gaubicher, T. Le Mercier, Y. Chabre, J. Angenault, and M. Quarton, *J. Electrochem. Soc.* **146,** 4375 (1999).
4. J. Gaubicher, F. Orsini, T. Le Mercier, S. Llorente, A. Villesuzanne, J. Angenault, and M. Quarton, *J. Solid State Chem.* **150,** 250 (2000).
5. A. Manthiram and J. B. Goodenough, *J. Power Sources* **26,** 403 (1989).
6. A. Nadiri, C. Delmas, R. Salmon, and P. Hagenmuller, *Rev. Chim. Miner.* **21,** 537 (1984).
7. J. Gaubicher, G. Vaughan, C. Masquelier, C. Wurm, J. Angenault, Y. Chabre, L. Nazar, and M. Quarton, 10th Int. Meeting on Lithium Batteries, Como, Italy, May–June 2000.
8. A. Manthiram and J. B. Goodenough, *Solid State Ionics* **71,** 349 (1987).
9. A. K. Padhi, K. S. Nanjundaswamy, and J. B. Goodenough, *J. Electrochem. Soc.* **144,** 1188 (1997).
10. M. Touboul, E. Le Samedi, and M. Quarton, *J. Less-Common Met.* **146,** 67 (1989).
11. J. De Meulenaer and H. Tompa, *Acta Crystallogr., Sect. A: Found Crystallogr.* **19,** 1014 (1965).
12. T. Debaerdemaeker, G. Germain, P. Main, L. S. Refaat, C. Tate, and M. M. Woolfson. "MULTAN 88, Computer programs for the automatic solution of crystal structures from X-ray diffraction data," Universities of York, England and Louvain, Belgium, 1988.
13. W. R. Busing, *Acta Crystallogr., Sect. A: Found Crystallogr.* **27,** 683 (1971).
14. "International Tables for X-Ray Crystallography," Vol. IV, Kynoch Press, Birmingham, England, 1974.
15. P. J. Becker and P. Coppens, *Acta Crystallogr., Sect. A: Found Crystallogr.* **31,** 417 (1975).
16. R. D. Shannon, *Acta Crystallogr., Sect. A: Found Crystallogr.* **32,** 751 (1976).
17. S. C. Abrahams and J. L. Bernstein, *J. Chem. Phys.* **45,** 2745 (1966).
18. M. Touboul and M. Quarton, *Acta Crystallogr. Sect. C: Cryst. Struct. Commun.* **44,** 1887 (1988).
19. S. B. Yu, C. P. Wang, E. P. Day, and R. H. Holm, *Inorg. Chem.* **30,** 4067 (1991).
20. F. Neveu, N. Gaultier, N. Korber, J. Jaud, and P. Castan, *J. Chem. Soc. Dalton Trans.* 4005 (1995).
21. O. Kahn, *in* "Molecular Magnetism," VCH, Weinhem, Germany, 1993.
22. D. P. Kessissoglou, W. M. Butler, and V. L. Pecoraro, *Inorg. Chem.* **26,** 495 (1987).
23. M. D. Carducci and R. J. Doedens, *Inorg. Chem.* **28,** 2494 (1989).
24. F. Sudreau, D. Petit, and J. P. Boilot, *J. Solid State Chem.* **83,** 78 (1989).